Translational Diffusion of Macromolecules and Nanoparticles Modeled as Non-overlapping Bead Arrays in an Effective Medium

Stuart Allison,* Hongxia Pei, Margaret Haynes, Yao Xin, Lydia Law, Josh Labrum, and Daphne Augustin

Department of Chemistry, Georgia State University, P.O. Box 4098, Atlanta, Georgia 30302-4098

Received: November 8, 2007; In Final Form: February 16, 2008

There are three objectives to the present work. First, starting from a boundary element (BE) formulation of low Reynolds number hydrodynamics, model the translational diffusion of macromolecules modeled as an array of non-overlapping beads, and show how this approach is equivalent to previous formulations of "bead hydrodynamics" and under what conditions. Second, show how this approach can be improved upon by accounting for the variation in forces over the surfaces of individual beads and also extending the approach to a gel modeled as an effective medium, EM. Third, develop a "combined obstruction and hydrodynamic effect" model of the translational diffusion of irregularly shaped macromolecules in a gel. In one of the cases studied, the BE approach is shown to be equivalent to previous "bead model" formulations in which intersubunit hydrodynamic interaction is modeled using the Rotne−Prager tensor. A bead model that accounts for the variation in hydrodynamic stress forces over the individual bead surfaces is shown to be in best agreement with exact results for simple bead arrays made up of 2−4 subunits. The translational diffusion of rods, modeled as strings of from 2 to 100 touching beads in dilute gels is examined. Interpolation formulas valid over a range of gel concentrations and rod lengths are derived for the parallel and perpendicular components of the diffusion tensor as well as the orientationally averaged diffusion tensor. The EM model accounts for the long-range hydrodynamic interaction exerted by the gel support matrix on the diffusing particle of interest but does not account for the reduction in diffusion caused by the direct obstruction of the gel, or steric effect. Both effects are accounted for by writing the translational diffusion in a gel as the product of two terms representing long-range hydrodynamic interaction and steric effects. Finally, the diffusion of a 564 base pair DNA in a 2% agarose gel is examined and model results are compared to experiment (Pluen, A.; Netti, P. A.; Jain, R. K.; Berk, D. A. *Biophys. J.* **1999**, *77*, 542−552). For reasonable choices of model parameters, fair agreement between theory and experiment is achieved.

I. Introduction

Over the past 20 years, there has been growing interest in the diffusion of macromolecules and nanoparticles in a congested or porous medium. This includes a wide variety of different environments and applications such as diffusion in the cytoplasm of cells,[1] concentrated suspensions,[2] gels or hydrogels,[3−10] and mucus.[11] What is driving this interest is that it is relevant to the transport of macromolecules and drugs in living tissue and also in the broad field of separation technology. The diffusion of a host particle through a rigid gel matrix is reduced, relative to diffusion in "free solution", by long-range hydrodynamic interaction and short-range steric effects. These two effects can be considered separately,[3] and that strategy is followed in the present work. Brownian dynamics has proven to be a useful way of dealing with short-range steric effects by explicitly modeling the migration of a particle through a gel matrix.[2,12] However, the long-range nature of hydrodynamic interaction has proven difficult to deal with when the congested "background" is accounted for explicitly.[13] Computational methods involving periodic boundary conditions show promise in this regard.[14]

A simpler way of dealing with the contribution of long-range hydrodynamic interaction makes use of the effective medium, EM, model originally developed by Brinkman,[15] and Debye and Bueche.[16] In the EM model, the "fluid" surrounding the particle of interest, which includes both solvent and the "gel" support medium, is treated as a hydrodynamic continuum. As discussed in the next section, a special screening term is added to the external force/volume on the fluid in the low Reynolds number Navier−Stokes equation that accounts for the presence of a gel, and the resulting equation is called the Brinkman equation. Starting from a microscopic model, where the support medium consists of uniform segments, Felderhof and Deutch were able to derive the Brinkman equation as a mean field approximation.[17] The EM model has been applied with some success to the diffusion of particles (modeled as spheres) in gels[3,4] and the electrophoretic stretch of duplex DNA in gels.[18,19] Recently, the gel electrophoresis of spherical particles[20] and non-overlapping bead arrays[21] was studied within the framework of the EM model. In the present work, the EM model is applied to the translational diffusion of structures represented by non-overlapping bead arrays.

Detailed modeling of the sedimentation and diffusion of macromolecules represented by bead arrays was carried out by a number of groups in the late 1970s.[22−27] Today, much of the "bead hydrodynamics" modeling carried out makes use of the software program *HYDROPRO*[28,29] that has its roots in this earlier work. It should be emphasized, however, that this

* Corresponding author. Phone: 404-413-5519; e-mail: sallison@gsu.edu.

10.1021/jp710700n CCC: $40.75
Published on Web 04/17/2008

modeling is carried out in free solution without the presence of a gel support medium. In order to account for the presence of a gel modeled as an effective medium, EM, we shall turn to the boundary element, BE, approach.[30] Although the BE approach has not been as widely used as the "bead method" in studying diffusion and sedimentation in free solution,[22−29] its use is growing.[31−33] It has also been recognized that the BE approach is more general and starts from essentially exact expressions.[34] This has made it possible to model more complex transport phenomenon such as electrophoresis[35−37] and electroviscosity[38] of irregularly shaped model macromolecules. In addition, the BE method makes it possible to test long-held assumptions, and an example of that shall be given in the present work with regards to the variation over a bead surface of the hydrodynamic force exerted by a bead on the surrounding fluid.

The outline of this paper is as follows. In the Theory section, the BE procedure is applied to a macromolecule/particle modeled as an array of non-overlapping beads translating through an EM fluid. In the absence of a gel support medium, it is shown under what circumstances our results reduce to those of earlier studies. We also show how the methodology can be modified to account, to lowest order, for the variation in hydrodynamic forces over the surfaces of individual beads. In Part A of the Applications section, the diffusion of some simple bead arrays in the absence of a gel is examined. Three different cases are considered and one of these is equivalent to "bead hydrodynamics" at the level of the Rotne−Prager tensor.[39] The most refined case, Case C, accounts for the variation in the hydrodynamic force/area exerted by the bead on the fluid. The results of the three formulations are compared with the exact results. In Part B, we extend the methodology to a dilute gel modeled as an EM and examine the diffusion of straight rod bead arrays for the same three cases as Part A. Interpolation formulas valid over a range of gel concentrations and rod lengths are derived for $D_{||}$, $D_{\perp}$, and D_{ave}. The EM model takes approximate account of the long-range hydrodynamic interaction exerted by the gel support matrix on the diffusing particle of interest but does not account for the retardation that occurs as a result of the direct obstruction the gel matrix causes.[3,4] Section C of the Applications section deals with this steric effect and draws on the considerable efforts of past investigations. How the combined effects of long-range hydrodynamic and short-range steric interactions influence diffusion is also dealt with in this section. In Section D, we examine the diffusion of a 564 base pair DNA in a 2% agarose gel and compare experiment[4] with modeling. In modeling, the DNA is represented as a rigid rod or wormlike chain of 78 touching beads. Account is taken of both long-range hydrodynamic (through EM modeling) and steric effects. For reasonable choices of model parameters, fair agreement between theory and experiment is achieved. In the Summary, the main points of this work and directions for future study are discussed.

II. Theory

The fluid is assumed to obey the Brinkman[15] and solvent incompressibility equations defined by

$$\eta\nabla^2\mathbf{v}(\mathbf{x}) - \nabla p(\mathbf{x}) = \eta\lambda^2\mathbf{v}(\mathbf{x}) \quad (1)$$

$$\nabla\cdot\mathbf{v}(\mathbf{x}) = 0 \quad (2)$$

where η is the solvent viscosity, $\mathbf{v}(\mathbf{x})$ is the local fluid velocity at point $\mathbf{x}$, p is the local pressure, and λ (units of 1/length) is the gel screening parameter. The hydraulic, or Darcy permeability, κ,[3,4] is simply related to λ by the relation $\kappa = 1/\lambda^2$. The term on the right-hand side of eq 1 represents an external force/unit volume due to the viscous drag on the fluid produced by the presence of the gel. In general, other external forces on the fluid may be present as well.[36] Most commonly, these arise as a result of electrostatic interactions. If, for example, the particle of interest is a macroion in an aqueous salt solution, then there will be an excess of counterions close to the macroion and the interaction of these ions with electric fields (either from the macroion itself or, if present, an external field). In the present work, we are interested in the phenomenon of translational diffusion where no external electric fields are present. Although electrical forces can, in principle, influence the diffusion of macroions through the mechanism of dielectric[40] and electrolyte[41−44] friction, these effects are small unless the macroion is highly charged and the ambient salt concentration is low.[44] In the present work, these external forces on the fluid shall be ignored.

In a recent analysis employing the boundary element method, a general expression was derived for the fluid (field point, $\mathbf{y}$, in fluid domain) or particle ($\mathbf{y}$ inside a bead) velocity of a bead array translating with uniform velocity, $\mathbf{u}$, through an effective medium that obeys eqs 1 and 2.[21] It should be emphasized that the field point, $\mathbf{y}$, can be chosen anywhere in space. In the "no salt" and "no electrical force" limit, which is a good assumption as discussed in the previous paragraph, eq B11 of ref 21 reduces to

$$\mathbf{v}(\mathbf{y})\,\Phi(\mathbf{y},V_e) + \sum_{J=1}^{N}\mathbf{u}\Phi(\mathbf{y},V_J) = \sum_{J=1}^{N}\int_{S_J}\mathbf{U}(\mathbf{r})\cdot\mathbf{f}(\mathbf{x})\,dS_{\mathbf{x}} + \eta\lambda^2\sum_{J=1}^{N}\mathbf{u}\cdot\int_{S_J}(\mathbf{x}-\mathbf{x}_J)(\mathbf{U}(\mathbf{r})\cdot\mathbf{n}(\mathbf{x}))dS_{\mathbf{x}} \quad (3)$$

where V_e denotes the fluid domain (exterior to all beads), V_J denotes the space occupied by bead J, $\Phi(\mathbf{y}, V)$ equals 1 if $\mathbf{y}$ lies within V, equals 0 if $\mathbf{y}$ lies outside of V, and equals 1/2 if $\mathbf{y}$ lies on the surface that just encloses V, the sum extends over all N beads comprising the bead array, $\mathbf{f}(\mathbf{x})$ represents the hydrodynamic force/area at $\mathbf{x}$, exerted by a particular bead on the fluid, $\mathbf{x}_J$ is the position of the center of bead J, $\mathbf{n}(\mathbf{x})$ is the outward surface unit normal at $\mathbf{x}$, $\mathbf{r} = \mathbf{x} - \mathbf{y}$

$$\mathbf{U}(\mathbf{r}) = \frac{w_1}{6\pi\eta}\mathbf{I} + \frac{1}{4\pi\eta\lambda^2}\left\{[3\nu_3 - 3w_3 - 3\lambda w_2 - \lambda^2 w_1]\left[\frac{1}{r^2}\mathbf{rr} - \frac{1}{3}\mathbf{I}\right]\right\} \quad (4)$$

$$w_n = \frac{e^{-\lambda r}}{r^n} \quad (5)$$

$$\nu_n = \frac{1}{r^n} \quad (6)$$

$\mathbf{I}$ is the 3 by 3 identity tensor, and $\mathbf{rr}$ is the 3 by 3 position tensor. Other quantities have been defined previously. In deriving eq 3 it was also assumed that "stick" boundary conditions hold. In other words, $\mathbf{v}(\mathbf{x}) = \mathbf{u}$ for $\mathbf{x}$ located at the surface of any bead.

It is useful to consider several averages of eq 4 over first one sphere of radius a', and then a second average over a second sphere of radius a as depicted in Figure 1. The center-to-center

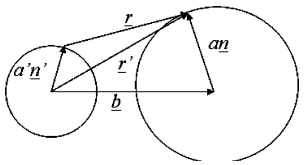

Figure 1. Two beads. The center-to-center vector is **b** and the radii are a' and a. Vectors $\mathbf{n}'$ and $\mathbf{n}$ denote outward unit normals from the bead centers to points on their surface.

vector is called **b** and it is assumed that $b = |\mathbf{b}| \geq (a + a')$. Averaging eq 4 over S'

$$\langle \mathbf{U}(\mathbf{r}) \rangle_{S'} = \frac{i_0(\lambda\, a')w_1}{6\pi\eta}\,\mathbf{I} + \frac{1}{4\pi\eta\lambda^2}\left\{[3\nu_3 - i_0(\lambda a')[3w_3 + 3\lambda w_2 + \lambda^2 w_1]]\left[\frac{1}{r'^2}\,\mathbf{r}'\mathbf{r}' - \frac{1}{3}\,\mathbf{I}\right]\right\} \quad (7)$$

In eq 7, the argument of w_n and υ_n terms is $r' = |\mathbf{r}'|$ and $i_0(z) = \sinh(z)/z$. A second average over S yields

$$\langle\langle \mathbf{U}(\mathbf{r}) \rangle_{S'} \rangle_S = \frac{i_0(\lambda\, a)\, i_0(\lambda\, a')w_1}{6\pi\eta}\,\mathbf{I} + \frac{1}{4\pi\eta\lambda^2}\left\{[3\nu_3 - i_0(\lambda\, a)\, i_0(\lambda\, a')[3w_3 + 3\lambda w_2 + \lambda^2 w_1]]\left[\frac{1}{b^2}\,\mathbf{bb} - \frac{1}{3}\,\mathbf{I}\right]\right\} \quad (8)$$

In eq 8, the argument of w_n and υ_n is $b = |\mathbf{b}|$. It should be emphasized that eqs 7 and 8 are exact. In the limit of no gel ($\lambda \rightarrow 0$), eq 8 can be written

$$\langle\langle \mathbf{U}(\mathbf{r}) \rangle_{S'} \rangle_S = \frac{1}{8\pi\eta\, b}\left\{\left[\mathbf{I} + \frac{1}{b^2}\,\mathbf{bb}\right] + \frac{a^2 + a'^2}{3b^2}\left[\mathbf{I} - \frac{3}{b^2}\,\mathbf{bb}\right]\right\} \quad (\lambda \rightarrow 0) \quad (9)$$

This, however, is just the Rotne−Prager tensor.[39] Another useful approximation to eq 8 is obtained by considering the case where $\lambda\, a$ and $\lambda\, a'$ are small. Under these conditions

$$i_0(\lambda\, a)\, i_0(\lambda\, a') \cong 1 + \frac{\lambda^2}{6}\,(a^2 + a'^2) \quad (10)$$

As a concrete example, consider a bead model for DNA where the subunit size is $a = 1.225$ nm in an agarose gel of concentration 0.020 gm/mL at 20 °C. Under these conditions, $\lambda = 0.173$ and $\lambda\, a = 0.212$ nm^{-1}.[21] In this example, the right- and left-hand sides of eq 10 agree to within 0.01% of each other. A much simpler averaging procedure involves expanding eq 4 in a quadratic polynomial about $r = b$ and then averaging over S and S'. In this approximate treatment, $i_0(\lambda\, a)\, i_0(\lambda\, a')$ in eq 8 is replaced with the right-hand side of eq 10. On the basis of the above discussion, this should be an excellent approximation. In what follows, we shall use the procedure of evaluating the "isotropic" part of eq 4 (first term on the right-hand side) exactly and the "anisotropic" part (second term of the right-hand side) using the quadratic expansion approximation. Evaluation of the "isotropic" term averages have been discussed previously in a study of the electrophoretic mobility of bead arrays.[45]

Next, return to eq 3, which should be exact subject to the assumptions that the fluid obeys eqs 1 and 2 and obeys "stick" hydrodynamic boundary conditions. At this point, we shall make an assumption common to that of previous investigations of the low Reynolds number translation of a bead array in a viscous fluid.[22−29] For a surface point, x, on the surface of bead J

$$\mathbf{f}(\mathbf{x}) \cong \frac{\mathbf{F}_J}{S_J} \quad (11)$$

where $\mathbf{F}_J$ is the average hydrodynamic force exerted by bead J on the surrounding fluid, $S_J = 4\pi a_J^2$ is the surface area of bead J, and a_J is the radius. For the special case of the translation of a single bead in the absence of a gel, eq 11 is exact (see Chapter 4 of ref 31). However, for a multibead array, this is not the case. We shall return to this point later. In applying eq 3, there is some flexibility in choosing **y**. In Case A, set $\mathbf{y} = \mathbf{x}_K$ (center of bead K). Making use of eq 11 and carrying out the averaging procedures outlined above yields

$$\mathbf{u}_K = \sum_{J=1}^{N} [\mathbf{C}_{KJ}^{(A)} \cdot \mathbf{u}_J + \mathbf{H}_{KJ}^{(A)} \cdot \mathbf{F}_J^{(A)}/\zeta_J] \quad (12)$$

where $\zeta_J = 6\pi\eta a_J$

$$\mathbf{C}_{KJ}^{(A)} = \begin{cases} \frac{2}{3}(1 - e^{-\lambda a_K}(1 + \lambda\, a_K))\mathbf{I} \quad (K = J) \\ \frac{2}{9}\lambda^3 a_J^3 i_0(\lambda\, a_J)\, k_0(\lambda\, x_{KJ})\mathbf{I} + \left[\frac{2}{3}\lambda^3 a_J^3 i_2(\lambda\, a_J)\, k_2(\lambda\, x_{KJ}) - \frac{1}{3}\,a_J^3\left(3\nu_3 - \left(1 + \frac{\lambda^2 a_J^2}{10}\right)(3w_3 + 3\lambda w_2 + \lambda^2 w_1)\right)\right] \left[\frac{1}{x_{KJ}^2}\,\mathbf{x}_{KJ}\mathbf{x}_{KJ} - \frac{1}{3}\,\mathbf{I}\right] \quad (K \neq J) \end{cases} \quad (13)$$

$$\mathbf{H}_{KJ}^{(A)} = \begin{cases} e^{-\lambda a_K}\mathbf{I} \quad (K = J) \\ \lambda a_J i_0(\lambda\, a_J)\, k_0(\lambda\, x_{KJ})\mathbf{I} + \frac{3a_J}{2\lambda^2}\left[3\nu_3 - \left(1 + \frac{\lambda^2 a_J^2}{6}\right)(3w_3 + 3\lambda w_2 + \lambda^2 w_1)\right] \left[\frac{1}{x_{KJ}^2}\,\mathbf{x}_{KJ}\mathbf{x}_{KJ} - \frac{1}{3}\,\mathbf{I}\right] \quad (K \neq J) \end{cases} \quad (14)$$

In eqs 13−14, i_n and k_n are modified spherical Bessell functions. Specifically, $i_0(z) = \sinh(z)/z$, $i_2(z) = \sinh(z)/z - 3\cosh(z)/z^2 + 3\sinh(z)/z^3$, $k_0(z) = e^{-z}/z$, $k_2(z) = e^{-z}(1/z + 3/z^2 + 3/z^3)$. Also, $x_{KJ} = |\mathbf{x}_{KJ}| = |\mathbf{x}_K - \mathbf{x}_J|$ and the argument of the υ_n and w_n terms above is x_{KJ} (see eqs 5 and 6). In eq 12, all of the $\mathbf{u}_J$ values are equal in the case of a translating bead array. The indices are included for clarity.

A different result is obtained if y is chosen to be some point on the surface of bead K (instead of at the bead center) and the result is subsequently averaged over all points on the surface of S_K. The result is Case B

$$\mathbf{u}_K = \sum_{J=1}^{N} [\mathbf{C}_{KJ}^{(B)} \cdot \mathbf{u}_J + \mathbf{H}_{KJ}^{(B)} \cdot \mathbf{F}_J^{(B)}/\zeta_J] \quad (15)$$

$$\mathbf{C}_{KJ}^{(B)} = \begin{cases} \frac{1}{3\lambda\, a_K}[(\lambda\, a_K - 1) + e^{-2\lambda a_K}(\lambda\, a_K + 1)]\mathbf{I}\ (K = J) \\ \frac{2}{9}\lambda^3 a_J^3 i_0(\lambda\, a_K)\left[i_0(\lambda\, a_J)k_0(\lambda\, x_{KJ})\mathbf{I} + 3i_2(\lambda\, a_J)\, k_2(\lambda\, x_{KJ})\left[\frac{1}{x_{KJ}^2}\,\mathbf{x}_{KJ}\mathbf{x}_{KJ} - \frac{1}{3}\,\mathbf{I}\right]\right] \\ -\left[\frac{1}{3}\,a_J^3\left(3\upsilon_3 - \left(1 + \lambda^2\left(\frac{a_K^2}{6} + \frac{a_J^2}{10}\right)\right)(3w_3 + 3\lambda w_2 + \lambda^2 w_1)\right] \left[\frac{1}{x_{KJ}^2}\,\mathbf{x}_{KJ}\mathbf{x}_{KJ} - \frac{1}{3}\,\mathbf{I}\right] \quad (K \neq J) \end{cases} \quad (16)$$

$$\mathbf{H}_{KJ}^{(B)}=\begin{cases} i_0(\lambda\, a_K)e^{-\lambda a_K}\mathbf{I}\ (K=J) \\ \lambda\, a_J i_0(\lambda a_K)\, i_0(\lambda\, a_J)\, k_0(\lambda\, x_{KJ})\mathbf{I}+ \\ \dfrac{3a_J}{2\lambda^2}\left[3\upsilon_3-\left(1+\dfrac{\lambda^2(a_J^2+a_K^2)}{6}\right)(3w_3+3\lambda w_2+\lambda^2 w_1)\right] \\ \qquad\left[\dfrac{1}{x_{KJ}^2}\mathbf{x}_{KJ}\mathbf{x}_{KJ}-\dfrac{1}{3}\mathbf{I}\right] \\ \qquad (K\neq J) \end{cases} \quad (17)$$

The typical procedure followed in a resistance problem[31] is to compute the elements of $\mathbf{C}_{KJ}$ and $\mathbf{H}_{KJ}$ once the geometry of a bead array is defined for either Cases A or B. Also, the bead velocities are specified, which in the case of translation involves translating them at a constant $\mathbf{u}$. Then eqs 12 or 15 are cast into "supermatrix" form

$$\mathbf{u}^* = \mathbf{C}^*\cdot\mathbf{u}^* + \mathbf{H}^*\cdot\mathbf{g} \quad (18)$$

where $\mathbf{u}^*$ and $\mathbf{g}$ are $3N$ by 1 column vectors in which elements $3K+1$ to $3K+3$ equal the components of $\mathbf{u}_K$ and $\mathbf{F}_K/\zeta_K$, respectively; $\mathbf{C}^*$ and $\mathbf{H}^*$ are $3N$ by $3N$ matrices made up of the elements of $\mathbf{C}_{KJ}$ and $\mathbf{H}_{KJ}$, respectively, for either model A or B. The $\mathbf{H}^*$ matrix is inverted to yield $\mathbf{H}^{-1}$. Solving eq 18 for $\mathbf{g}$

$$\mathbf{g} = \mathbf{H}^{-1}\cdot[\mathbf{I}_{3N} - \mathbf{C}^*]\cdot\mathbf{u}^* \quad (19)$$

where $\mathbf{I}_{3N}$ is the $3N$ by $3N$ identity matrix. The total force, $\mathbf{F}_{tot}$, exerted by the bead array of the fluid, is then related to the translational friction tensor, $\boldsymbol{\Xi}_t$, by

$$\mathbf{F}_{tot} = \sum_{J=1}^{N}\zeta_J\mathbf{g}_J = \boldsymbol{\Xi}_t\cdot\mathbf{u} \quad (20)$$

By translating the object along three orthogonal directions and computing the total forces in each case, it is straightforward to determine $\boldsymbol{\Xi}_t$. Finally, the components of the translational diffusion tensor, $\mathbf{D}_t$, are given, approximately, by

$$\mathbf{D}_t \cong k_B T\boldsymbol{\Xi}_t^{-1} \quad (21)$$

where k_B is Boltzmann's constant and $\boldsymbol{\Xi}_t^{-1}$ is the inverse of the friction tensor. (For general irregular rigid objects, there is a coupling between translation and rotation that has been well-documented.[13,31,46,47]) Although $\boldsymbol{\Xi}_t$ is independent of the choice of origin, $\mathbf{D}_t$ is not and this renders eq 21 approximate. For axisymmetric objects, eq 21 is exact. Even for detailed 20 base pair duplex DNA models that possess "propeller-like" symmetry and hence a definite coupling between translation and rotation, eq 21 is off by only 0.1%.[48] For most structures, it can be concluded that translation−rotation coupling is small and in the present work, eq 21 is used to estimate $\mathbf{D}_t$.)

Cases A and B discussed previously yield different $\mathbf{D}_t$ values, and examples are given in the main body of this work. Subject to the assumptions that the fluid obeys eqs 1 and 2 and that "stick" boundary conditions hold, eq 3 is exact and we might initially expect eqs 12 and 15 to be exact as well, but they are different. On going from eq 3 to eqs 12 or 15, one assumption and one approximation were made. The assumption was eq 11, and the approximation was a quadratic expansion of the anisotropic term of $\mathbf{U}$ as discussed following eq 10. Provided $\lambda\, a_J$ is small, a condition that is readily satisfied in the cases of interest in the present work, this latter approximation is expected to be a very good one as discussed previously. This leaves the assumption that $\mathbf{f}(\mathbf{x})$ is uniform over any given bead. Other investigators are certainly aware of the limitations of this assumption, particularly with regard to the rotational motion of bead arrays.[49] For translation, a common approach is to replace a single large bead with an array of smaller beads making the assumption implicit in eq 11, on average, more accurate.[50] The objective of the remainder of this section is deriving a first-order correction to eq 11. In doing so, we seek a more accurate solution without abandoning a relatively simple model.

The force/area, $\mathbf{f}$, is related to the hydrodynamic stress tensor, $\boldsymbol{\sigma}$, by[30]

$$\mathbf{f}(\mathbf{x}) = -\boldsymbol{\sigma}(\mathbf{x}+\Delta\mathbf{n}(\mathbf{x}))\cdot\mathbf{n}(\mathbf{x}) \quad (22)$$

where $\mathbf{n}(\mathbf{x})$ is the local outward unit normal to the particle surface at point $\mathbf{x}$, on the particle surface, and $\mathbf{x}+\Delta\mathbf{n}(\mathbf{x})$ is a point just in the fluid domain ($0<\Delta\ll$ bead radius). The stress tensor, in turn, is related to the local pressure, p, and fluid velocity, $\mathbf{v}$, by[13,31]

$$\boldsymbol{\sigma} = -p\mathbf{I} + \eta(\nabla\mathbf{v} + \nabla\mathbf{v}^T) \quad (23)$$

where $(\nabla\mathbf{v})_{ij} = \nabla_i v_j$ and $\nabla\mathbf{v}^T$ is the transpose of $\nabla\mathbf{v}$. It is straightforward to derive a boundary element expression for $\mathbf{f}(\mathbf{x})$ in the fluid domain using eq 3 and eqs 22−23. Expressions for $\nabla\mathbf{v}$ and $\nabla\mathbf{v}^T$ are obtained by differentiating eq 3 directly. For the pressure, we have from eq 1, $\nabla p = \eta\nabla^2\mathbf{v} - \eta\lambda^2\mathbf{v}$. Thus, it is straightforward to determine ∇p and then p by subsequent integration. This approach yields for a field point, $\mathbf{y}$, located in the fluid domain directly adjacent to bead K with outward unit normal $\mathbf{n}'(\mathbf{y})$

$$\begin{aligned} f_i(\mathbf{y}) = \sum_{j,k=1}^{3}\Big[n_j'(\mathbf{y})\int_{S_K} dS_x\sigma_{ij}'^{k}(\mathbf{r})\, f_k(\mathbf{x}) + \\ \eta\,\lambda^2 n_j'(\mathbf{y})u_{Kk}\int_{V_K} dV_x\sigma_{ij}'^{k}(\mathbf{r})\Big] + \\ \sum_{J\neq K=1}^{N}\left[\sum_{j,k=1}^{3}\Big[n_j'(\mathbf{y})\int_{S_J} dS_x\sigma'^{k}_{ij}(\mathbf{r})\Big) f_k(\mathbf{x}) + \right. \\ \left.\eta\,\lambda^2 n_j'(\mathbf{y})u_{Jk}\int_{V_J} dV_x\sigma_{ij}'^{k}(\mathbf{r})\Big]\right] \end{aligned} \quad (24)$$

In eq 24, $\mathbf{r} = \mathbf{x} - \mathbf{y}$, the i, j, k indices refer to Cartesian components, and J and K refer to bead indices. Also

$$\begin{aligned} \sigma_{ij}'^{k}(\mathbf{r}) = -\frac{\upsilon_3\delta_{ij}r_k}{4\pi} + \frac{1}{4\pi\lambda^2}\{h_1(r_i\delta_{jk}+r_j\delta_{ik}) + h_2(r_i\delta_{jk}+ \\ r_j\delta_{ik}+2r_k\delta_{ij}) - 2h_3 r_i r_j r_k\} \end{aligned} \quad (25)$$

where υ_3 is given by eq 6 (of argument r), δ_{ij} is the Kronecker delta, and

$$h_1 = 3\upsilon_5 - 3w_5 - 3\lambda w_4 - 2\lambda^2 w_3 - \lambda^3 w_2 \quad (26a)$$

$$h_2 = 3\upsilon_5 - 3w_5 - 3\lambda w_4 - \lambda^2 w_3 \quad (26b)$$

$$h_3 = 15\upsilon_7 - 15w_7 - 15\lambda w_6 - 6\lambda^2 w_5 - \lambda^3 w_4 \quad (26c)$$

In eq 26, the w_n values are given by eq 5 and the argument of the h and w values is r.

To motivate an *estimation* of the variation in $\mathbf{f}$ over a particular bead (bead K) using eq 24, we anticipate that the variation is due primarily to the presence of neighboring beads. For the J ≠ K terms in eq 24, approximate $\sigma_{ij}'^{k}(\mathbf{r})$ with $\sigma_{ij}'^{k}(\mathbf{x}_{JK})$. Equation 24 becomes

$$f_i(\mathbf{y}) \cong f_i^{(\mathrm{K})}(\mathbf{y}) + \sum_{j,k=1}^{3} \sum_{\mathrm{J}\neq K=1}^{N} n_j'(\mathbf{y}) \sigma_{ij}'^{k}(\mathbf{x}_{\mathrm{JK}}) [F_{\mathrm{Jk}} + \eta \lambda^2 V_{\mathrm{J}} u_{\mathrm{Jk}}] \tag{27}$$

The first term on the right-hand side of eq 24 is $f_i^{(\mathrm{K})}$. If eq 27 is averaged over S_{K}, then the second term on the right-hand side of eq 27 completely vanishes and we must have

$$\frac{F_{\mathrm{K}i}}{S_K} = \langle f_i(\mathbf{y}) \rangle_{S_{\mathrm{K}}} = \langle f_i^{(\mathrm{K})}(\mathbf{y}) \rangle_{S_{\mathrm{K}}} \tag{28}$$

Approximating the first term on the right-hand side of eq 27 with its average over surface S_{K}, we obtain

$$f_i(\mathbf{y}) \cong \frac{F_{\mathrm{K}i}}{S_{\mathrm{K}}} + \sum_{j,k=1}^{3} \sum_{\mathrm{J}\neq K=1}^{N} n_j'(\mathbf{y}) \sigma_{ij}'^{k}(\mathbf{x}_{\mathrm{JK}}) [F_{\mathrm{Jk}} + \eta \lambda^2 V_{\mathrm{J}} u_{\mathrm{J}k}] \tag{29}$$

Comparing eqs 11 and 29 above, it can be seen that in deriving eqs 12 and 15 only the first term on the right-hand side of eq 29 was included. If the correction term is also included, then we can write (for Case A)

$$\mathbf{u}_{\mathrm{K}} = \sum_{J=1}^{N} [\mathbf{C}_{\mathrm{KJ}}^{(\mathrm{A})} \cdot \mathbf{u}_{\mathrm{J}} + \mathbf{H}_{\mathrm{KJ}}^{(\mathrm{A})} \cdot \mathbf{F}_{\mathrm{J}}^{(\mathrm{A})} / \zeta_J] + \delta \mathbf{u}_{\mathrm{K}} \tag{30}$$

It is straightforward, but tedious, to evaluate δu_{K}. Before writing down a formal expression for this correction, it is useful to define a number of terms

$$\chi_{\mathrm{J}} = \frac{a_{\mathrm{J}}^4}{2\zeta_J \lambda^4} \tag{31a}$$

$$B_{Jm} = F_{Jm} + \eta \lambda^2 V_{\mathrm{J}} u_{Jm} \tag{31b}$$

$$\alpha_{KJ} = 3 - \left(3w_0(x_{\mathrm{KJ}}) + 3\lambda w_{-1}(x_{\mathrm{KJ}}) + \frac{3}{2}\lambda^2 w_{-2}(x_{\mathrm{KJ}})\right) \tag{31c}$$

$$\beta_{KJ} = \frac{1}{2}\lambda^2 w_{-2}(x_{\mathrm{KJ}}) \tag{31d}$$

$$\gamma_{KJ} = \lambda^3 w_{-3}(x_{\mathrm{KJ}}) \tag{31e}$$

$$\zeta_{KJ}^{(1)} = \frac{2\alpha_{KJ} - \gamma_{KJ}}{x_{\mathrm{KJ}}^4} \tag{31f}$$

$$\zeta_{KJ}^{(2)} = \frac{\alpha_{KJ} + \beta_{KJ}}{x_{\mathrm{KJ}}^4} \tag{31g}$$

$$\zeta_{KJ}^{(3)} = \frac{10\alpha_{KJ} + 6\beta_{KJ} - 2\gamma_{KJ}}{x_{\mathrm{KJ}}^4} \tag{31h}$$

$$\Omega_{KJLim} = \frac{(\mathbf{x}_{\mathrm{JK}})_i (\mathbf{x}_{\mathrm{LJ}})_m}{x_{\mathrm{KJ}} x_{\mathrm{JL}}} \tag{31i}$$

$$\Omega_{KJL}^0 = \sum_{i=1}^{3} \Omega_{KJLii} \tag{31j}$$

With these terms, the general expression of $\delta \mathbf{u}_{\mathrm{K}i}$ can be written

$$\delta u_{\mathrm{K}i} = \sum_{\mathrm{J}\neq K=1}^{N} \chi_J \sum_{\mathrm{L}\neq J=1}^{N} \sum_{\mathrm{m}=1}^{3} B_{\mathrm{L}m} \Big[\zeta_{KJ}^{(1)} \zeta_{JL}^{(1)} (\Omega_{KJLmi} + \Omega_{KJL}^0 \delta_{im}) + 2\zeta_{KJ}^{(2)} \zeta_{JL}^{(1)} \Omega_{KJLim} + \zeta_{KJ}^{(3)} \zeta_{JL}^{(1)} \Omega_{KJKim} \Omega_{KJL}^0 + \zeta_{KJ}^{(1)} \zeta_{JL}^{(3)} \Omega_{JLJim} \Omega_{KJL}^0 - \zeta_{KJ}^{(2)} \zeta_{JL}^{(3)} \Omega_{KJLim} + \frac{1}{2} \zeta_{KJ}^{(3)} \zeta_{JL}^{(3)} \Omega_{KJLim} (\Omega_{KJL}^0)^2 \Big] \tag{32}$$

Although complicated in appearance, the terms appearing in eq 32 are evaluated rapidly and efficiently by a computer. Because forces appear in eq 32 through the $B_{\mathrm{L}m}$ terms (eq 31b) and yet these are unknown quantities, the problem is solved iteratively. In the first iteration, $\delta \mathbf{u}_{\mathrm{K}}$ is set to zero and an initial estimate of the forces is then obtained following the procedure of eqs 18 and 19. These are then used in eq 32 to obtain $\delta \mathbf{u}_{\mathrm{K}}^{(1)}$. Next, define the $3N$ by 1 column vector, $\mathbf{u}^*$, in which elements $3K + 1$ to $3K + 3$ equal the three components of $\mathbf{u}_{\mathrm{K}} - \delta \mathbf{u}_{\mathrm{K}}^{(1)}$. Equations 18 and 19 are used again to obtain revised forces, and then eq 32 is used to obtain $\delta \mathbf{u}_{\mathrm{K}}^{(2)}$. This procedure is repeated until the forces converge to within a predefined tolerance level. (In the present work, the tolerance level is a relative change in average absolute force of 10^{-6}. This is usually achieved in fewer than five iterations.)

This section shall be ended by summarizing its key results for the special case of no gel ($\lambda \rightarrow 0$). Under these conditions, all $\mathbf{C}_{\mathrm{KJ}}^{(\mathrm{A})}$ and $\mathbf{C}_{\mathrm{KJ}}^{(\mathrm{B})}$ terms vanish. Also, $\mathbf{H}_{\mathrm{KK}}^{(\mathrm{A})}$ and $\mathbf{H}_{\mathrm{KK}}^{(\mathrm{B})}$ equal $\mathbf{I}$. For $\mathrm{K} \neq \mathrm{J}$

$$\mathbf{H}_{\mathrm{KJ}}^{(\mathrm{A})} = \frac{3a_{\mathrm{J}}}{4x_{\mathrm{JK}}} \left(\mathbf{I} + \frac{1}{x_{\mathrm{JK}}^2} \mathbf{x}_{\mathrm{JK}} \mathbf{x}_{\mathrm{JK}} \right) - \frac{3a_{\mathrm{J}}^3}{4x_{\mathrm{JK}}^3} \left(\frac{1}{x_{\mathrm{JK}}^2} \mathbf{x}_{\mathrm{JK}} \mathbf{x}_{\mathrm{JK}} - \frac{1}{3} \mathbf{I} \right) \tag{33}$$

$$\mathbf{H}_{\mathrm{KJ}}^{(\mathrm{B})} = \frac{3a_{\mathrm{J}}}{4x_{\mathrm{JK}}} \left(\mathbf{I} + \frac{1}{x_{\mathrm{JK}}^2} \mathbf{x}_{\mathrm{JK}} \mathbf{x}_{\mathrm{JK}} \right) - \frac{3a_{\mathrm{J}}(a_{\mathrm{J}}^2 + a_{\mathrm{K}}^2)}{4x_{\mathrm{JK}}^3} \left(\frac{1}{x_{\mathrm{JK}}^2} \mathbf{x}_{\mathrm{JK}} \mathbf{x}_{\mathrm{JK}} - \frac{1}{3} \mathbf{I} \right) \tag{34}$$

The correction to account for variation in $\mathbf{f}$ over the surface of an individual bead (eq 32) reduces to

$$\delta u_{\mathrm{K}i} = -\frac{3}{4} \sum_{\mathrm{J}\neq K=1}^{N} \frac{a_{\mathrm{J}}^4}{\zeta_J x_{\mathrm{KJ}}^3} \sum_{\mathrm{L}\neq J=1}^{N} \frac{1}{x_{\mathrm{JL}}^3} \left(1 - 3 \frac{(\mathbf{x}_{\mathrm{JK}} \cdot \mathbf{x}_{\mathrm{LJ}})^2}{x_{\mathrm{JK}}^2 x_{\mathrm{LJ}}^2} \right) \sum_{m=1}^{3} (\mathbf{x}_{\mathrm{JK}})_i (\mathbf{x}_{\mathrm{LJ}})_m F_{\mathrm{L}m} \tag{35}$$

III. Applications

A. Diffusion of Simple Bead Arrays in the Absence of an EM or Gel. In the previous section, we discussed two boundary element cases, A and B, which arise depending on the choice of field point, $\mathbf{y}$. In Case A, the field point is chosen to lie at the center of a particular bead, and in Case B, an average is carried out over all points on the surface of the particular bead. In the limit of no gel, Case B reduces to the standard result[22−29] in which the intersubunit hydrodynamic interaction is represented by the Rotne−Prager tensor.[39] A common assumption made in bead hydrodynamics is that the hydrodynamic force exerted by a bead on the surrounding fluid, $\mathbf{f}(\mathbf{x})$, is uniform over the bead surface, where $\mathbf{x}$ is a point on the bead surface. In the present work, this approximation is relaxed in what we call Case C. Specifically, Case C is Case A corrected to account, to lowest order, for the variation in $\mathbf{f}(\mathbf{x})$ over the bead surface.

TABLE 1: Diffusion of Bead Arrays[a] ($\lambda = 0$)

structure	orientation	$D^{(A)}$	$D^{(B)}$	$D^{(C)}$	D_{exact}[b]
dimer	parallel	1.063	1.024	1.004	0.977
"	perpendicular	0.889	0.906	0.886	0.870
"	average[c]	0.945	0.945	0.925	0.906
trimer (linear)	parallel	0.986	0.970	0.979	0.935
"	perpendicular	0.793	0.811	0.793	0.784
"	average[c]	0.857	0.864	0.855	0.835
tetramer (linear)	parallel	0.954	0.928	0.935	0.897
"	perpendicular	0.728	0.745	0.728	0.723
"	average[c]	0.804	0.806	0.797	0.781
tetramer (square)	in plane	0.969	0.960	0.932	0.894
"	out of plane	0.829	0.858	0.829	0.794
"	average[c]	0.922	0.926	0.898	0.861

[a] All diffusion constants are divided by those of a single sphere of volume equal to that of the corresponding bead array. [b] From ref 51. [c] $D_{ave} = (2D_{\perp} + D_{||})/3$ or $(2D_{in\ plane} + D_{out\ of\ plane})/3$.

Summarized in Table 1 are reduced (dimensionless) translational diffusion constants of simple bead arrays along different orientations for Cases A through C and also exact results.[51] All diffusion constants are divided by those of a sphere of equal volume, D_{eqv}. For a bead array made up of N identical beads of radius a, $D_{eqv} = (k_BT/(6\pi\eta a))N^{-1/3}$. Cases A and B compare about equally well with the exact results. Case C is clearly superior to the other two, and this is to be expected because the assumption of uniform $\mathbf{f}(\mathbf{x})$ over an individual bead is relaxed. Also note that D_{exact} always lies lower than model D values in the examples considered in Table 1. This is generally true on the basis of energy dissipation arguments.[39] This is also true for translational diffusion of bead arrays in an EM where $\lambda > 0$.

B. Diffusion of Straight Rod Bead Arrays in an Effective Medium, EM. The translational diffusion constant of a *sphere* in an EM, D_s, of radius R_h can be written[18]

$$\left(\frac{D_s^{ng}}{D_s}\right)_{EM} = 1 + \lambda R_h + \frac{1}{9}\lambda^2 R_h^2 \qquad (36)$$

In eq 36, $D_s^{ng} = k_BT/(6\pi\eta R_h)$ is the translational diffusion constant of the sphere in the absence of a gel ($\lambda = 0$). For arbitrary bead arrays, the diffusion tensor defined by eq 21 can be diagonalized and let Λ_j denote one of these diagonal components. In the special case of an axisymmetric particle such as a linear array of beads in a reference reference frame with the x axis parallel to the line passing through the centers of the beads, Λ_1 corresponds to the diffusion constant parallel to the bead array (long) axis and Λ_2 or Λ_3 the diffusion constant perpendicular to the bead array (long) axis. In general, we might expect Λ_j to exhibit a similar dependence on gel concentration. (Gel concentration enters through the parameter λ.[17,18,20,21] We shall return to this point in the next section.) Using eq 36 as a guide, define

$$X_j = \frac{1}{\gamma}\left(\left(\frac{\Lambda_j^{ng}}{\Lambda_j}\right)_{EM} - 1\right) = a_{0j} + a_{1j}\gamma + a_{2j}\gamma^2 \qquad (37)$$

$$\gamma = \lambda R_h = \frac{\lambda k_B T}{6\pi\eta D_{ave}^{ng}} \qquad (38)$$

$$D_{ave}^{ng} = \frac{1}{3} Tr[\mathbf{D}^{ng}] = \frac{1}{3}\sum_{j=1}^{3} \Lambda_j^{ng} \qquad (39)$$

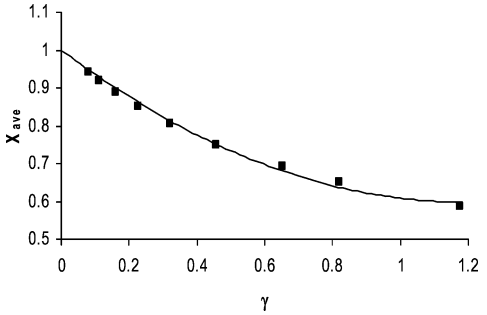

Figure 2. X_{ave} vs γ for a linear array of 100 identical touching beads. This figure illustrates, in a specific case, how D_{ave} (effective medium) of a long rod varies with gel concentration. Conditions are a (bead radii) = 1.225 nm, T = 20 °C, η = 1.002 cp, γ (dimensionless) is defined by eq 38.

TABLE 2: Gel Parameters, $a_{sj}^{(m)}$, for Rods of Touching Beads

model	orientation (j)	s	$a_{sj}^{(0)}$	$a_{sj}^{(1)}$	$a_{sj}^{(2)}$
A	|| (1)	0	.946	−.0843	.00790
"	"	1	.196	−.116	−.00310
"	"	2	.0594	−.0405	.0151
"	⊥ (2 or 3)	0	1.012	.0759	−.00630
"	"	1	.315	−.0969	−.0398
"	"	2	.104	−.170	.0591
"	ave	0	1.000	.000	.000
"	"	1	.289	−.143	−.0178
"	"	2	.0584	−.0845	.0363
B	|| (1)	0	.977	−.0882	.0080
"	"	1	.193	−.100	−.0064
"	"	2	.0118	−.0160	.0117
"	⊥ (2 or 3)	0	.994	.0719	−.0056
"	"	1	.249	−.0853	−.0392
"	"	2	.0301	−.121	.0522
"	ave	0	1.000	.000	.000
"	"	1	.245	−.121	.0205
"	"	2	.0031	−.0528	.0319
C	|| (1)	0	.919	−.0695	.0059
"	"	1	.103	−.0587	.0114
"	"	2	.0656	−.0426	.0152
"	⊥ (2 or 3)	0	.979	.0933	−.0087
"	"	1	.279	−.0739	−.0430
"	"	2	.108	−.171	.0593
"	ave	0	1.00	.000	.000
"	"	1	.250	−.119	−.0213
"	"	2	.0572	−.0836	.0361

In addition to the individual components, eq 37 can be applied to the orientationally averaged diffusion constant, $D_{ave} = (\Lambda_1 + \Lambda_2 + \Lambda_3)/3$. We have investigated the low gel concentration ($0 < \gamma < 0.5$) dependence of the Λ_j for rods made up of from $N = 2$ to 100 touching beads. We choose parameters appropriate for DNA in low salt aqueous media at 20 °C:[21] a = 1.225 nm, η = 1.002 cp. Shown in Figure 2 is X_{ave} versus γ for the N = 100 case (720 base pair duplex DNA modeled as a straight rod). Similar plots for parallel and perpendicular components as well as different N values exhibit similar behavior. The a_{sj} parameters are obtained by least-squares fitting to a quadratic polynomial. The a_{sj} values, in turn, can be well fit with the following polynomial

$$a_{sj} = a_{sj}^{(0)} + a_{sj}^{(1)}\ln(N) + a_{sj}^{(2)}(\ln(N))^2 \qquad (40)$$

The resulting coefficients for rods of touching beads are given in Table 2 for Models A, B, and C for parallel, perpendicular, and "average" orientations. When plotted, differences between the three models are small. It should be mentioned that the orientationally averaged a_0 values all lie close to 1 and are independent, or nearly so, of N. The same behavior is also seen

for rings of touching beads (results not shown). From the polynomial coefficients in Table 2, it is straightforward to account for the relative effect of the EM on the diffusion constant of a rodlike particle.

C. Connecting Translational Diffusion in an EM to That in a Gel. Modeling the diffusion of a single sphere in a gel has been treated extensively in the past.[3,4,52,53] There have been numerous investigations in this regard, and it is beyond the scope of the present study discuss these in detail. Amsden[53] gives a particularly thorough summary of past work and compares theory and experiment for a wide variety of different gels, particle sizes, and models. In Amsden's terminology, we follow the strategy of a "combined obstruction and hydrodynamics effect" model. What is new about the present work is that it extends modeling to account for irregularly shaped particles. The present approach should, however, be applicable even when the gel concentration is high.

In a gel, two factors reduce the translational diffusion constant, D, over its value in the absence of a gel, D^{ng}, in the "combined obstruction and hydrodynamics effect" strategy.[53] One of these is long-range hydrodynamic interaction that the gel exerts on the diffusing particle of interest. The EM (effective medium) model accounts for this long-range effect, on average. The other factor is a steric effect, S, which accounts for the domain of the fluid excluded to penetration by the diffusing particle of interest. The relative diffusion constant can be written as a product of these two terms[3,4]

$$\frac{D}{D^{ng}} = \left(\frac{D}{D^{ng}}\right)_{EM} S(\phi_{ex}) \tag{41}$$

where the EM subscript denotes the diffusion constant ratio within the framework of the EM model and ϕ_{ex} is the volume fraction of fluid excluded to the diffusing particle of interest. The ratio, $(D/D^{ng})_{EM}$ is determined by the procedure outlined in Section II. For spherical particles of radius a, the steric function can be readily deduced from Ogston[54] and closely related[55] theory

$$S(\phi_{ex}) \approx \frac{1}{1+\dfrac{2\phi_{ex}}{3}} \approx e^{-0.667\phi_{ex}} = e^{-0.667(1+a/\sigma)^2\phi} \tag{42}$$

where σ is the hydrated radius of a gel segment and ϕ denotes the volume of hydrated gel material divided by the total volume. Equation 42 is similar to a steric function that works well over a broad range of ϕ_{ex} but restricted to spherical particles[56]

$$S(\phi_{ex}) = \exp[-0.84\phi_{ex}^{1.09}] \tag{43}$$

Brownian dynamics simulations of the electrophoresis of short rodlike particles in dilute gels represented as a cubic lattice of gel fibers are well described by steric functions of the general form of eqs 42 and 43.[57] In the present case, eq 43 shall be used. In general, we compute ϕ_{ex} by a sampling procedure in which a single model bead array is placed, at random, in an EM consisting of straight gel fibers oriented along three orthogonal directions that are chosen at random.[21] In principle, these gel fibers may be crosslinked, but that is not done explicitly in the present work. In a subroutine, (EXVOL), of our main program, this procedure is repeated 100 to 10 000 times with different gel fiber environments and, if our model particle is flexible, different array conformations. The fraction of configurations that produce no overlap between the macromolecule and the gel then gives us an estimate of ϕ_{ex}.

The gel is typically characterized by its chemical composition (agarose or polyacrylamide, fo example), its weight concentration, M (typically in g of dry gel material/total volume), and possibly the concentration of crosslinker if any is present.[58] To make contact with the λ parameter of eq 1, use is first made of the relation[17]

$$n_s\zeta_s = \eta\lambda^2 = \frac{\eta}{\kappa} \tag{44}$$

where n_s is the number density of gel segments (assumed uniform in composition), ζ_s is the friction coefficient of a gel segment (radius $= \sigma$), η is the solvent viscosity, and κ is the hydraulic permeability. Accounting for the hydrodynamic interaction between gel segments[18]

$$\zeta_s = 6\pi\eta\sigma\left(1+\lambda\sigma+\frac{1}{9}\lambda^2\sigma^2\right) \tag{45}$$

Let ρ_g denote the dry weight density of gel material (which equals 1.64 gm/mL for agarose[59]), ω_s the ratio of dry gel volume to hydrated gel volume (which equals 0.625 for agarose[52]), and ϕ the volume fraction of hydrated gel. The weight concentration, M, of gel can be related to these other parameters by

$$M = \rho_g\omega_s\phi = \frac{4}{3}\pi\rho_g\omega_s n_s\sigma^3 \tag{46}$$

Substituting eqs 45 and 46 into eq 44 and solving for λ yields

$$\lambda = \frac{A}{2\sigma}\left(1+\sqrt{\frac{5}{9}+\frac{4}{A}}\right)\Big/\left(1-\frac{A}{9}\right) \tag{47}$$

where $A = 9M/(2\rho_g\omega_s)$. The concentration dependence of λ given by eq 47 can be compared to a correlation derived by Jackson and James[60]

$$\frac{1}{\lambda^2} = -\frac{3r_f^2}{20\phi}(\ln(\phi)+0.931) \tag{48}$$

where r_f is the "fiber radius" of the gel. Despite differences, eqs 47 and 48 are in good agreement with each other over the concentration range $0.005 < M < 0.03$ provided one sets $r_f = 0.61\ \sigma$.

D. Comparison of Modeling and Experiment for a 564 bp Duplex DNA in a 2% Agarose Gel. Because the focus of the present work is diffusion of irregularly shaped particles modeled as bead arrays, we would like to end this work with an example that clearly illustrates the potential usefulness of this approach. Duplex DNA diffusion in agarose gels fulfils our need.[4,5,8,11] In the experimental studies, the method of choice is fluorescence recovery after photobleaching, FRAP, and the studies have been restricted to fairly long DNA in the 0.5 to 10.0 kilo-base size range. Because of their large size, we shall focus on only the shortest DNA, which is a 564 base pair fragment.[4]

To represent duplex DNA, a straight rigid rod, once broken rod, or discrete wormlike chain model[61,62] shall be considered. Current consensus places the hydrodynamic radius, R, (viewing duplex DNA on a local distance scale as a right circular cylinder) at 1.0 ± 0.1 nm.[63,64] Following Hagerman,[61,62] one sets the contour length, L, equal to $2Na$ where N is the number of touching contiguous beads and "a" is the bead radius. Setting the volume of a model circular cylinder, πR^2L, equal to that of N touching beads, $4\pi a^3N/3$, gives $a = (3/2)^{(1/2)}R = 1.225$ nm. The number of base pairs equals $7.2N$ and to model a 564 base

TABLE 3: D/D_{eqv} for Different DNA Models with Different σ

model	σ (nm)	D^{ng}/D_{eqv}	D/D_{eqv}
straight rod	1.6	.266	.0432
"	2.0	"	.0519
"	2.4	"	.0607
broken rod	1.6	.264	.0391
"	2.0	"	.0471
"	2.4	"	.0555
wormlike chain	1.6	.277	.0405
"	2.0	"	.0489
"	2.4	"	.0559

pair DNA, $N = 78$. For a straight rigid rod or once broken rigid rod, only a single conformation needs to be considered. For a discrete wormlike chain, a single chain conformation is generated using random numbers and this procedure is equivalent to selecting a single chain conformation from an equilibrium distribution.[61,62] The translational diffusion tensor, **D**, can then be computed for this particular chain and diagonalized to yield Λ_j ($j = 1-3$). Average Λ_j values are then obtained by simple averaging over an "ensemble" of independent chains. An "ensemble" of 100 chains is sufficient in the present work to determine $<\Lambda_j>$ to an accuracy of better than 2%. For the persistence length, P, of DNA, a value of 50 nm is assumed[65] when DNA is modeled as a discrete wormlike chain.

The experiments of Pluen et al.[4] were carried out at 298 K in a 0.1 M phosphate buffered saline solution with $\eta = 0.87$ cp. In the absence of a gel, a log(D^{ng}) versus log(N) plot (Figure 3 of ref 4) gives a straight line and from this we deduce that $D^{ng} = 1.3 \times 10^{-11}$ m^2/s for 564 base pair DNA. When corrected for temperature and viscosity, this value is entirely consistent with D^{ng} values measured by dynamic light scattering for DNA fragments in the same size range.[66] For the same fragment in 2% agarose, Pluen et al.[4] report $D = 1.9 \pm 0.1 \times 10^{-12}$ m^2/s. The translational diffusion constant of a sphere of volume equal to that of a 78 bead model ($a = 1.225$ nm) appropriate for 564 base pair DNA at 298 K and $\eta = 0.87$ cp is $D_{eqv} = 4.80 \times 10^{-11}$ m^2/s. In units of D_{eqv}, experiment then gives $D^{ng} = 0.271$ and $D = 0.040 \pm 0.002$. In modeling, we set $\rho_g = 1.64$ gm/cm^3, $\omega_s = 0.625$ (following eq 45), and obtain the results summarized in Table 3 (D values are in units of D_{eqv}) for the three models: a straight rigid rod, a once broken rod (pivot point in the middle with a bend angle of 90°), and a discrete wormlike chain with $P = 50$ nm. Also, only the results are presented for Case B (see Results, Part A) because those for the other two cases are very similar for a 78 bead model.

Several points need to be made regarding a comparison between theory and experiment. In the absence of a gel, agreement is seen to be excellent. It is also worth noting that D^{ng} is relatively insensitive to conformation. The model studies show a slightly greater conformation dependence of D in 2% agarose. Good agreement between modeling and experiment is also observed in 2% agarose provided $\sigma = 1.6$ nm. When a larger value of σ is used in modeling, modeling overestimates D relative to experiment. At first glance, a value of σ as small as 1.6 nm may not seem unreasonable because low-angle X-ray scattering shows evidence of a substantial population of gel fibers with a radius of 1.5 nm and a smaller population with a significantly larger diameter.[67] (For a detailed summary of the structure of agarose gels, see ref 52.) However, earlier studies of the electrophoresis of Au nanoparticles in agarose gel were well fit using σ in the 2.0−2.4 nm range.[20] We need to proceed with caution for several reasons. First, the steric function given by eq 44 is strictly valid for spherical particles[56] although it works for short rods as well.[57] Using it for rods or wormlike chains as long as those used here will require further testing. Second, direct interactions between the diffusing particle and the gel have not been included in modeling. Agarose is known to contain low levels of sulfate ions,[68] and direct electrostatic interactions are known to influence the diffusion of charged species in gels.[7,69] In the present case, carrying out the experiment in 0.1 M salt has undoubtedly minimized that interaction,[4] but it needs to be considered in general. Finally, there is also evidence that the detailed structure of an agarose gel depends on the rate of cooling used in its preparation.[7]

These cautionary remarks aside, it is clear that modeling is able to largely account for the substantial reduction in the rate of translational diffusion of a 564 base pair DNA when placed in a 2% agarose gel.

Summary. The objectives of this work are threefold. First, starting from a boundary element, BE, formulation of low Reynolds number hydrodynamics, model the translational diffusion of macromolecules modeled as an array of nonoverlapping beads, and show how this approach is equivalent to previous formulations[22−29] and under what conditions. Second, show how this approach can be improved upon by accounting for the variation in forces over the surfaces of individual beads and also extending the approach to a gel modeled as an effective medium, EM. Third, develop a "combined obstruction and hydrodynamic effect" model to the translational diffusion of irregularly shaped macromolecules in a gel and give a preliminary example of its application. The Theory section addresses the formal aspects of the first two objectives. In what we call Case B, the BE approach is shown to be equivalent to previous "bead model" formulations in which intersubunit hydrodynamic interaction is modeled using the Rotne−Prager tensor.[39] Three cases (including Case B) are compared to exact results for simple bead arrays in the absence of an EM in Part A of the Applications section. Case C, which accounts for the variation in hydrodynamic stress over the bead surfaces, is shown to be in best agreement with the exact results. In Part B of the Applications section, the diffusion of rods in dilute gels is examined. The rods are modeled as linear strings of touching beads ranging in number from 2 to 100. Interpolation formulas valid over a range of gel concentrations and rod lengths are derived for the parallel and perpendicular components of the diffusion tensor as well as the orientationally averaged diffusion tensor. The EM model accounts for the long-range hydrodynamic interaction exerted by the gel support matrix on the diffusing particle of interest but does not account for the reduction in diffusion caused by the direct obstruction of the gel. Part C of the Applications section deals with how long-range hydrodynamic interaction and the steric effect of the gel[3,4,52−56,60] can be accounted for simultaneously. In Section D, we examine the diffusion of a 564 base pair DNA in a 2% agarose gel and compare experiment[4] with modeling. In modeling, the DNA is represented as a rigid rod or wormlike chain of 78 touching beads.[61,62] For reasonable choices of model parameters, fair agreement between theory and experiment is achieved.

It would be straightforward to extend the present work to rotational diffusion. This was not done in the present work because we felt a need to focus on the subject of translational diffusion in gels, and indeed it is in this area where we feel our approach will have the greatest impact in future study. More work is needed with regard to the steric function, $S(\phi_{ex})$ (see eq 44), for irregularly shaped particles. A straightforward way to approach this is Brownian dynamics simulation[57] of model bead arrays in explicit models of gel matrices.[70] Work along

these lines is currently underway in our laboratory. Also, past experiments of the translational diffusion of DNA[4,5,8,11] or other polymers in gels[71] involve long chains of many monomer units. For flexible structures, it is necessary to examine many conformations ($\geq$100) and invert a 3N by 3N matrix for each (N = number of beads making up a model). On computational grounds, this limits one to models made up of no more than approximately 150 beads. For duplex DNA modeled as a string of touching beads,[61,62] 150 beads are equivalent to 1080 base pairs, and this represents an approximate upper bound in modeling. In the study of the translational diffusion of long polymers in gels, lower resolution Rouse−Zimm models[72,73] or models intermediate in their level of detail between touching bead[61,62] and Rouse−Zimm chains[74] could be considered. For DNA or other polymers that are much longer than the fiber spacing in the gel, it might be difficult to model transport explicitly. In these cases, reptation theories may be more appropriate.[75] Finally, there is a great need for more quantitative experimental work of DNA and other polymers of variable length in gels of variable concentration.

References and Notes

(1) Zimmerman, S. B.; Minton, A. *Annu. Rev. Biophys. Biomolec. Struct.* **1993**, *22*, 27−65.
(2) Dwyer, J. D.; Bloomfield, V. A. *Biophys. J.* **1993**, *65*, 1810−1816.
(3) Johnson, E. M.; Berk, D. A.; Jain, R. K.; Deen, W. M. *Biophys. J.* **1996**, *70*, 1017−1026.
(4) Pluen, A.; Netti, P. A.; Jain, R. K.; Deen, W. M. *Biophys. J.* **1999**, *77*, 542−552.
(5) Pernodet, N.; Tinland, B.; Sturm, J.; Weil, G. *Biopolymers* **1999**, *50*, 45−59.
(6) Sass, H. -J.; Musco, G.; Stahl, S. J.; Wingfield, P. T.; Grzesiek, S. *J. Biomolecular NMR* **2000**, *18*, 303−309.
(7) Fatin-Rouge, N.; Starchev, K.; Buffle, J. *Biophys. J.* **2004**, *86*, 2710−2719.
(8) Tatarkova, S. A.; Berk, D. A. *Phys. Rev. E* **2005**, *71*, 41913-1 − 41913-5.
(9) Hirota, N.; Kumaki, Y.; Narita, T.; Gong, J. P.; Osada, Y. *J. Phys. Chem. B* **2000**, *104*, 9898−9903.
(10) Fatin-Rouge, N.; Milon, A.; Buffle, J. *J. Phys. Chem. B* **2003**, *107*, 12126−12137.
(11) Shen, H.; Hu, Y.; Saltzmann, W. M. *Biophys. J.* **2006**, *91*, 639−644.
(12) Castelnovo, M.; Grauwin, S. *Biophys. J.* **2007**, *92*, 3022−3031.
(13) Happel, J.; Brenner, H. *Low Reynolds Number Hydrodynamics*; Martinus Nijhoff, The Hague: Boston, MA, 1983; Chapter 8.
(14) Felderhof, B. U. *Physica A* **1989**, *159*, 1−18.
(15) Brinkman, H. C. *Appl. Sci. Res. A* **1947**, *1*, 27−34.
(16) Debye, P.; Bueche, A. M. *J. Chem. Phys.* **1948**, *16*, 573−579.
(17) Felderhof, B. U.; Deutch, J. M. *J. Chem. Phys.* **1975**, *62*, 2391−2397.
(18) Stigter, D. *Macromolecules* **2000**, *33*, 8878−8889.
(19) Feree, S.; Blanch, H. W. *Biophys. J.* **2004**, *87*, 468−475.
(20) Allison, S. A.; Xin, Y.; Pei, H. *J. Colloid Interface Sci.* **2007**, *313*, 328−337.
(21) Allison, S. A.; Pei, Y.; Xin, Y. *Biopolymers* **2007**, *87*, 102−114.
(22) McCammon; J. A., Deutch, J. M. *Biopolymers* **1976**, *15*, 1397−1408.
(23) Nakajima, H.; Wada, Y. *Biopolymers* **1977**, *16*, 875−893.
(24) Garcia de la Torre, J.; Bloomfield, V. A. *Biopolymers* **1977**, *16*, 1747−1763, 1765−1778, 1779−1793.
(25) Schmitz, K. S. *Biopolymers* **1977**, *16*, 2635−2640.
(26) Teller, D. C.; Swanson, E.; de Haen, C. *Methods Enzymol.* **1979**, *61*, 103−124.
(27) Garcia de la Torre, J.; Bloomfield, V. A. *Quart. Rev. Biophys.* **1981**, *14*, 81−139.
(28) Garcia de la Torre, J.; Huertas, M. L.; Carrasco, B. *Biophys. J.* **2000**, *78*, 719−730.
(29) Garcia de la Torre, J. *Biophys. Chem.* **2001**, *93*, 159−170.
(30) Youngren, G. K.; Acrivos, A. *J. Fluid Mech.* **1975**, *69*, 377−403.
(31) Kim, S.; Karilla, S. J. *Microhydrodynamics*; Butterworth-Heinemann: Boston, MA, 1991.
(32) Aragon, S. R. *J. Comput. Chem.* **2004**, *25*, 1191−1205.
(33) Aragon, S. R.; Hahn, D. K. *Biophys. J.* **2006**, *91*, 1591−1603.
(34) Wegener, W. A. *Biopolymers* **1986**, *25*, 627−637.
(35) Allison, S. A.; Nambi, P. *Macromolecules* **1992**, *25*, 3971−3978.
(36) Allison, S. A. *Macromolecules* **1996**, *29*, 7391−7401.
(37) Allison, S. A.; Carbeck, J. D.; Chen, C.; Burkes, F. *J. Phys. Chem. B* **2004**, *108*, 4516−4524.
(38) Allison, S. A. *Macromolecules* **1998**, *31*, 4464−4474.
(39) Rotne, J.; Prager, S. *J. Chem. Phys.* **1969**, *50*, 4831−4837.
(40) Hubbard, J; Onsager, L. *J. Chem. Phys.* **1977**, *67*, 4850−4857.
(41) Booth, F. *J. Chem. Phys.* **1954**, *22*, 1956−1968.
(42) Geigenmuller, U. *Chem. Phys. Lett.* **1984**, *110*, 666−667.
(43) Schurr, J. M. *Chem. Phys. Lett.* **1984**, *110*, 668, 470.
(44) Allison, S. A.; Chen, C.; Stigter, D. *Biophys. J.* **2001**, *81*, 2258−2268.
(45) Xin, Y.; Hess, R.; Ho, N.; Allison, S. A. *J. Phys. Chem. B* **2006**, *110*, 25033−25044.
(46) Garcia Bernal, J. M.; Garcia de la Torre, J. *Biopolymers* **1980**, *19*, 751−766.
(47) Garcia de la Torre, J.; Jimenez, A.; Freire, J. J. *Macromolecules* **1982**, *15*, 148−154.
(48) Mazur, S.; Chen, C.; Allison, S. A. *J. Phys. Chem. B* **2001**, *105*, 1100−1108.
(49) Garcia de la Torre, J.; Rodes, V. *J. Chem. Phys.* **1983**, *79*, 2454−2460.
(50) Garcia Bernal, J. M.; Garcia de la Torre, J. *Biopolymers* **1981**, *20*, 129−139.
(51) Swanson, E.; de Haen, C.; Teller, D. C. *J. Chem. Phys.* **1980**, *72*, 1623−1628.
(52) Johnson, E. M.; Berk, D. A.; Jain, R. K. *Biophys. J.* **1995**, *68*, 1561−1568.
(53) Amsden, B. *Macromolecules* **1998**, *31*, 8382−8395.
(54) Ogston, A. G. *Faraday Soc. Trans.* **1958**, *54*, 1754−1757.
(55) Tsai, D. S.; Streider, W. *Chem. Eng. Commun.* **1986**, *40*, 207−218.
(56) Johansson, L.; Lofroth, J. -E. *J. Chem. Phys.* **1993**, *98*, 7471−7479.
(57) Allison, S. A.; Li, Z.; Reed, D.; Stellwagen, N. C. *Electrophoresis* **2002**, *23*, 2678−2689.
(58) Dunn, M. J. *Electrophoresis: Proteins*; BIOS Scientific: Oxford, UK, 1993.
(59) Laurent, T. C. *Biochim. Biophys. Acta* **1967**, *136*, 199−205.
(60) Jackson, G. W.; James, D. G. *Can. J. Chem.* **1986**, *64*, 362−374.
(61) Hagerman, P. J.; Zimm, B. H. *Biopolymers* **1981**, *20*, 1481−1502.
(62) Hagerman, P. J. *Biopolymers* **1981**, *20*, 1503−1535.
(63) Eimer, W.; Williamson, J. R.; Boxer, S. G.; Pecora, R. *Biochemistry* **1990**, *29*, 799−811.
(64) Diaz, R.; Fujimoto, B. S.; Schurr, J. M. *Biophys. J.* **1997**, *72*, A322.
(65) Schellman, J. A.; Harvey, S. C. *Biophys. Chem.* **1995**, *55*, 95−114.
(66) Sorlie, S. S.; Pecora, R. *Macromolecules* **1990**, *23*, 487−497.
(67) Djabourov, M.; Clark, A. H.; Rowlands, D. W.; Murphy, S. B. *Macromolecules* **1989**, *22*, 180−188.
(68) Calladine, C. R.; Collis, C. M.; Drew, H. R.; Mott, M. R. *J. Mol. Biol.* **1991**, *221*, 981−1005.
(69) Fatin-Rouge, N.; Milon, A.; Buffle, J.; Goulet, R. R.; Tessier, A. *J. Phys. Chem. B* **2003**, *107*, 12126−12137.
(70) Mercier, J. -F.; Slater, G. W. *Macromolecules* **2001**, *34*, 3437−3445.
(71) Favre, E.; Leonard, M.; Laurent, A.; Dellacherie, E. *Colloids Surf., A* **2001**, *194*, 197−206.
(72) Rouse, P. E. *J. Chem. Phys.* **1953**, *21*, 1272−1280.
(73) Zimm, B. E. *J. Chem. Phys.* **1956**, *24*, 269−278.
(74) Allison, S. A. *SPIE: Photon Correlation Spectroscopy: Multicomponent Systems* **1991**, *1430*, 50−64.
(75) Zimm, B. H.; Levene, S. D. *Quart. Rev. Biophys.* **1992**, *25*, 171−204.